ЕҢБЕК ҚЫЗЫЛ ТУ ОРДЕНДІ
«Ә. Б. БЕКТҰРОВ АТЫНДАҒЫ
ХИМИЯ ҒЫЛЫМДАРЫ ИНСТИТУТЫ»
АКЦИОНЕРЛІК ҚОҒАМЫ

ҚАЗАҚСТАННЫҢ ХИМИЯ ЖУРНАЛЫ

ХИМИЧЕСКИЙ ЖУРНАЛ КАЗАХСТАНА

CHEMICAL JOURNAL of KAZAKHSTAN

АКЦИОНЕРНОЕ ОБЩЕСТВО
ОРДЕНА ТРУДОВОГО КРАСНОГО ЗНАМЕНИ
«ИНСТИТУТ ХИМИЧЕСКИХ НАУК
им. А. Б. БЕКТУРОВА»

3 (67)

ИЮЛЬ – СЕНТЯБРЬ 2019 г.

ИЗДАЕТСЯ С ОКТЯБРЯ 2003 ГОДА

ВЫХОДИТ 4 РАЗА В ГОД

АЛМАТЫ
2019

UDC 54.057; 546.763; 54.061; 54-165.3

M. M. MATAEV[1], G. S. PATRIN[2], K. Zh. SEITBEKOVA[1], Zh. Y. TURSINOVA[1], M. R. ABDRAIMOVA[1]

[1]Kazakh State Women's Teacher Training University, Almaty, Kazakhstan,
[2]Institute of Engineering Physics and Radio Electronics Siberian Federal University, Krasnoyarsk, Russia

SYNTHESIS AND X-RAY DIFFRACTION STUDY OF THE CHROMITE-MANGANITES

Abstracts. In this work synthesized new chromite-manganite phases using sol-gel method and their composition was studied by X-ray method. Chromium oxide, manganese oxide, yttrium oxide, metal carbonates, citric acid and glycerin were used as starting materials. It is shown that the use of citric acid and glycerol as precipitant, giving a positive effect to monophase samples. Precipitate was subjected to homogenizing roast in the temperature range from 600 to 1100°C, reaching the level of sintering samples were controlled by the basis of X-ray diffraction profiles. All the X-ray reflection lines have been successfully indexed according to the orthorhombic perovskite structure with space group: Pbnm (62) and with the following parameters: $Y_{(1-x)}MgCr_{0,5}Mn_{0,5}O_3$,(x≈0,7) –a=5.557, b=7.515, c=5.252 Å, Z = 4; $Y_{(1-x)}BaCr_{0,5}Mn_{0,5}O_3$, (x≈0,7) –a=9.102, b=5.533, c=7.330 Å, Z = 4; $Y_{(1-x)}SrCr_{0,5}Mn_{0,5}O_3$, (x≈0,7) –a=7.109, b=7.436, c=6.756 Å, Z = 4.

Keywords: chromium complex, sol-gel process, crystal structures, nanostructures, doping, X-ray diffraction.

Introduction. The increasing demand to reduce the dependency on fossil-fuels has necessitated advancements in device-related materials for alternative energy technologies. Solid oxide fuel cells (SOFCs) may play an important role in the future of energy technology, as they are able to produce energy by direct chemical-to-electrical conversion of oxygen and hydrogen or hydrocarbon fuels with high efficiency and relatively little emission of greenhouse gases [1, 2]. When operated in reverse, the fuelcell functions as an electrolyzer, effectively storing the energy obtained by splitting water into hydrogen and oxygen for futurepower generation [3]. Typically, SOFCs must be operated at high temperatures of around 800–1000°C, primarily in order to overcome the slowkinetics of the oxygen reduction reaction (ORR) ($O_2 + 4e^- \rightarrow 2O^{2-}$) at the cathode,which results in a high cathodic overpotentialat lower temperatures [4, 5]. Even at higher temperatures, the slow kinetics of the ORR is a major contributor to the overall resistance of the SOFC, resulting in decreased device efficiency [4]. High temperature operation of the SOFCcauses accelerated material degradation and high operational costs. A key material property that correlates with the ORRis the surface exchange coefficient k*, as higher k* values correspond to more rapid splitting of the O_2 and incorporation into the cathode, which in turn correlates with more efficient overall ORR. A cathode with a higher value of the surface exchange coefficient k* and correspondingly improved ORR activity would allow for lower temperature

operation of the SOFC, which in turn improves fuelcell lifetime by slowing material degradation. Such cathode improvements would increase the economic incentive for large scale commercialization of SOFC technology [5]. Perovskite oxides have presented themselves as the most promising alternative materials to precious metal alloys for SOFCs, [6–8] with materials such as $La_{1-x}Sr_xMnO_3$ (LSM) and $La_{1-x}Sr_xCo_{1-y}Fe_yO_3$ (LSCF) appearing widely in commercial SOFCs [8-10]. Similar perovskites also appear to be very promisingfor aqueous electrocatalysis, with materials such as $Ba_{1-x}Sr_xCo_{1-y}Fe_yO_3$ (BSCF) and $Pr_{1-x}Ba_xCoO_3$ displaying recordhigh ORR [11] and oxygen evolution reaction (OER) [12] activities, respectively. This work seeks to discover high activity perovskite cathode materials that are also stable under SOFC operating conditions.

EXPERIMENTAL

When using the sol-gel method, nanoparticles, porous structures with an ordered and disordered arrangement of pores, nano coatings, fiber and monolithic structures can be obtaining [13]. The process consists of the following stages:

Stage 1. Formation of sol. Hydrolysis and polycondensation of monomer compounds.

Stage 2. Formation of gel. At this stage, the formation of a spatial gel grid takes place. At the same time, there is a sharp increase in the viscosity of the solution. In an acidic environment, hydrolysis is faster than polycondensation. Therefore, in the initial stages, chains are mainly forming, and then there is a branching of chains and their cross-linking. Large spherical particles are forming in alkaline medium.

Stage 3. The aging of gel (syneresis). There is a seal structure of the gel, the compression of mesh and the selection of the gel solvent. This stage can take several days. First, separate particles of silicon oxide are forming in the system. Then their coalescence proceeds with the formation of large porous structures. Initially, a small number of pores with a large diameter are forming in the material. As the gel syneresis proceeds, the number of pores increases, and the pores become thinner.

Stage 4. Drying. The liquid is removing from the spatial structure of the gel. If the removal of solvent occurs in the supercritical conditions, the formed aerogel. If you carry out drying at an elevated temperature, a denser structure is formed- xerogel [13].

When using the sol-gel method, different types of nano composites can be synthesizing. For example, the scheme of the synthesis of nano composites such as "chromite – manganite's" is showing in figure 1.

The formation of new phases was controlled by the method of X-ray phase analysis produced by X-ray diffractometer Miniflex 600 (Rigaku) using CuK α-radiation filtered by the filter (U = 30 кV, J = 10 мА, the rotation speed of 1000 pulses per second, time constant = 5 sec., the range of angles 2θ from 5 to 900). Radiographs of the synthesized polycrystalline powders were indicated by

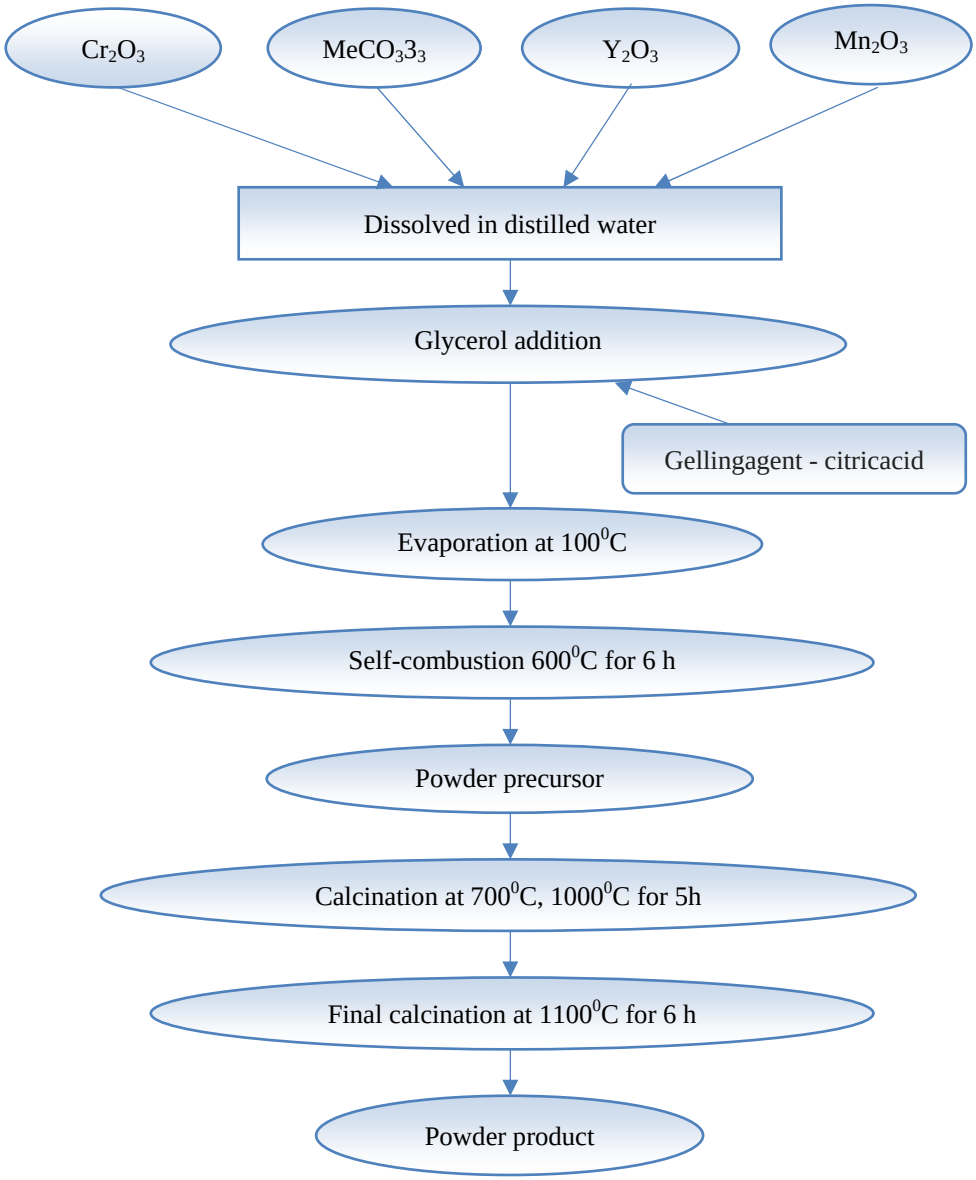

Figure 1 – Synthesis scheme for nanocomposites of chromite-manganites using the sol-gel method

the homology method (homologue is a distorted structure type of perovskite). The density of chrimite – manganites was determined by the pycnometric method according to GOST 2211-65. Toluene served as indifferent liquid. The density of the chromite – manganite's were measured 4–5 times and data were averaged [14].

RESULTS AND DISCUSSION

Powder X-ray diffraction patterns (refer with: figure 2a–c) show that the samples show single phase and indexed (refer with: table 1) in the cubic structure with Fm-3m (225) group space.

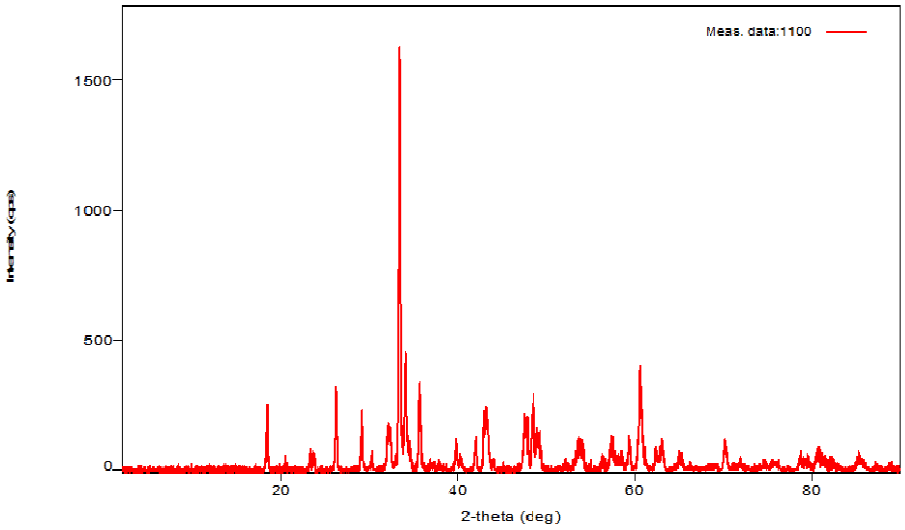

a) X-ray picture of powder $Y_{(1-x)}MgCr_{0,5}Mn_{0,5}O_3$,(x≈0,7)

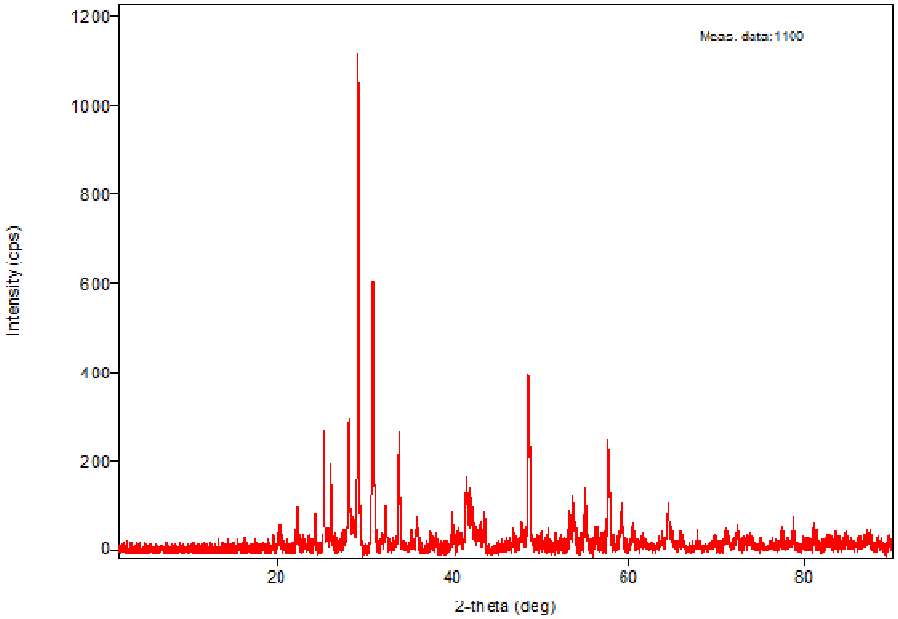

b) X-ray picture of powder $Y_{(1-x)}BaCr_{0,5}Mn_{0,5}O_3$, (x≈0,7)

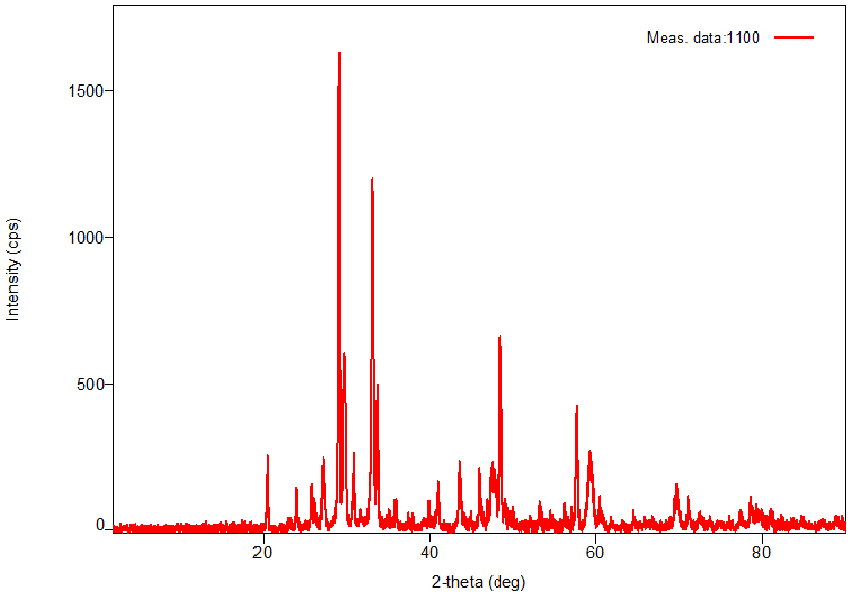

c) X-ray picture of powder $Y_{(1-x)}SrCr_{0,5}Mn_{0,5}O_3$,(x≈0,7)

Figure 2 – XRD patterns of perovskites chromite-manganites:
a) $Y_{(1-x)}MgCr_{0,5}Mn_{0,5}O_3$,(x≈0,7), б) $Y_{(1-x)}BaCr_{0,5}Mn_{0,5}O_3$, (x≈0,7), c) $Y_{(1-x)}SrCr_{0,5}Mn_{0,5}O_3$,(x≈0,7)

The data of the X-ray diffraction of the synthesized chromite-manganites are presented in table1.

Table 1 – Indexing of radiographs of synthesized phases

№	[°2Th.]	d[Å]	Int. [%]	$10^4/d^2$exp.	hkl	$10^4/d^2$teor.
1	2	3	4	5	6	7
$Y_{(1-x)}MgCr_{0,5}Mn_{0,5}O_3$,(x≈0,7)						
1	20.59	4.310	0.6	538.32	(0,1,1)	538.24
2	23.17	3.835	2.7	679.94	(1,0,1)	679.81
3	23.69	3.753	2.9	709.97	(0,2,0)	709.85
4	26.07	3.415	20.3	857.47	(1,1,1)	857.39
5	31.94	2.799	20.9	1276.42	(2,0,0)	1276.33
6	33.38	2.682	100.0	1390.22	(1,2,1)	1390.19
7	34.04	2.632	24.7	1443.54	(0,0,2)	1443.44
8	34.16	2.623	10.5	1453.46	(2,1,0)	1453.40
9	36.32	2.472	0.4	1636.45	(2,0,1)	1636.36
10	37.74	2.382	0.9	1762.45	(1,0,2)	1762.39
11	38.31	2.348	0.7	1813.86	(2,1,1)	1813.77

Continuation of table 1

1	2	3	4	5	6	7
12	39.67	2.270	3.8	1940.65	(1,1,2)	1940.56
13	39.86	2.260	2.2	1957.87	(0,3,1)	1957.79
14	40.15	2.244	2.2	1985.88	(2,2,0)	1985.81
15	41.89	2.155	5.5	2153.30	(0,2,2)	2153.22
16	43.13	2.095	8.3	2278.41	(1,3,1)	2278.35
17	43.82	2.064	2.2	2347.36	(2,2,1)	2347.28
18	45.04	2.011	0.6	2472.72	(1,2,2)	2472.66
19	47.37	1.918	18.8	2718.33	(2,0,2)	2718.25
20	48.47	1.877	14.3	2838.38	(0,4,0)	2838.27
21	48.78	1.866	7.6	2871.95	(2,3,0)	2871.87
22	48.99	1.858	11.9	2896.73	(2,1,2)	2896.68
23	51.94	1.759	2.2	3231.98	(3,0,1)	3231.87
24	53.04	1.725	0.6	3360.64	(1,3,2)	3360.55
25	53.46	1.713	14.8	3407.89	(3,1,1)	3407.81
26	54.39	1.686	0.6	3517.91	(1,4,1)	3517.87
27	54.78	1.674	0.5	3568.53	(1,0,3)	3568.48
$Y_{(1-x)}BaCr_{0,5}Mn_{0,5}O_3$, (x≈0,7)						
1	15.49	5.714	1.0	306.28	(1,0,1)	306.22
2	19.47	4.556	6.3	481.76	(2,0,0)	481.87
3	20.10	4.415	13.0	513.02	(0,1,1)	513.96
4	22.36	3.973	41.2	633.52	(1,1,1)	633.48
5	22.96	3.871	5.1	667.35	(2,0,1)	667.27
6	24.25	3.668	26.6	743.26	(0,0,2)	743.21
7	25.31	3.516	92.4	808.91	(2,1,0)	808.86
8	26.17	3.403	52.2	863.52	(1,0,2)	863.47
9	28.12	3.171	100.0	994.51	(2,1,1)	994.45
10	30.83	2.898	58.2	1190.70	(1,1,2)	1190.62
11	31.28	2.857	1.5	1225.12	(2,0,2)	1225.08
12	31.86	2.807	9.6	1269.15	(3,0,1)	1269.12
13	32.36	2.764	45.8	1308.95	(0,2,0)	1308.89
14	35.33	2.538	12.9	1552.44	(2,1,2)	1552.38
15	35.85	2.503	2.3	1596.17	(3,1,1)	1596.11
16	36.07	2.488	1.2	1615.47	(1,2,1)	1615.38
17	38.05	2.363	9.2	1790.90	(2,2,0)	1790.82
18	38.45	2.340	3.6	1826.28	(3,0,2)	1826.17
19	39.52	2.278	1.5	1927.05	(4,0,0)	1927.00

End of table 1

1	2	3	4	5	6	7
20	40.05	2.249	18.2	1977.06	(2,2,1)	1977.01
21	40.30	2.236	2.1	2000.12	(0,1,3)	2000.06
22	40.85	2.207	4.5	2053.03	(0,2,2)	2053.00
23	41.47	2.176	45.0	2111.94	(4,0,1)	2111.87
24	41.55	2.172	42.1	2119.73	(1,1,3)	2119.69
25	41.90	2.155	35.9	2153.30	(2,0,3)	2153.25
26	42.08	2.145	42.9	2173.42	(1,2,2)	2173.36
27	42.90	2.106	10.7	2254.67	(4,1,0)	2254.59
$Y_{(1-x)}SrCr_{0,5}Mn_{0,5}O_3$, (x≈0,7)						
1	16.40	5.400	3.1	342.93	(1,0,1)	342.87
2	17.61	5.031	7.9	395.08	(1,1,0)	395.03
3	18.07	4.904	3.0	415.81	(0,1,1)	415.77
4	20.37	4.357	1.1	526.77	(1,1,1)	526.72
5	20.69	4.290	0.1	543.35	(1,0,1)	543.28
6	23.98	3.708	2.5	727.31	(1,1,1)	727.26
7	24.12	3.688	19.1	735.22	(0,2,0)	735.18
8	25.87	3.441	62.6	844.56	(2,0,0)	844.52
9	27.14	3.283	5.5	927.80	(0,0,2)	927.72
10	27.42	3.250	100.0	946.74	(1,2,0)	946.67
11	28.60	3.118	14.7	1028.60	(2,1,0)	1028.53
12	29.05	3.071	0.5	1060.33	(-2,1,1)	1060.25
13	29.30	3.045	0.6	1078.51	(-1,2,1)	1078.44
14	29.76	2.999	74.4	1111.85	(0,1,2)	1111.78
15	29.91	2.985	30.7	1122.30	(-1,1,2)	1122.26
16	31.98	2.797	1.4	1278.24	(1,2,1)	1278.21
17	33.15	2.700	19.4	1371.74	(-2,0,2)	1371.68
18	34.24	2.616	0.1	1461.25	(2,1,1)	1461.19
19	34.99	2.562	7.8	1523.50	(1,1,2)	1523.45
20	35.37	2.535	17.2	1556.12	(-2,1,2)	1556.08
21	35.66	2.516	6.0	1579.71	(2,2,0)	1579.68
22	36.03	2.491	1.6	1611.58	(-2,2,1)	1611.53
23	36.74	2.444	2.5	1674.16	(-1,2,2)	1674.12
24	38.50	2.336	5.8	1832.54	(-3,0,1)	1832.46
26	38.87	2.315	1.0	1865.94	(1,3,0)	1865.89
27	39.09	2.302	8.3	1887.07	(0,3,1)	1887.01

The reliability of the indexing results is controlled by a satisfactory coincidence of experimental and calculated values of the inverse squares of the interplanar spacings ($10^4/d^2$), and the coincidence degree of the x-ray and miCrometrically densities values of the studied compounds.

The data of X-ray indexing of synthesized chromite-manganites show that they have an orthorhombic structure with the following parameters of elementary cells:

Table 2 – Phase symmetry, lattice parameters, unit cell volume, X-ray and pycnometric density of the chromite – manganites obtained by sol-gel method

№	Compound	Phase symmetry	a, Å	b, Å	c, Å	$V_{э.я.}$, Å^3	Z	$P_{X\text{-}ray}$	$P_{рус}$
1	$Y_{(1-x)}MgCr_{0,5}Mn_{0,5}O_3$,(x≈0,7)	orthorombic	5.557	7.515	5.252	219.3	4	5.76	5.75
2	$Y_{(1-x)}BaCr_{0,5}Mn_{0,5}O_3$, (x≈0,7)	orthorombic	9.102	5.533	7.330	369.1	4	4.55	4.54
3	$Y_{(1-x)}SrCr_{0,5}Mn_{0,5}O_3$, (x≈0,7)	orthorombic	7.109	7.436	6.756	347.6	4	3.95	3.94

Thus, nano composites such as "chromite – manganite's"were synthesizing by sol – gel method. Using the ceramic technology, considering the Tamman's conditions, the authors defined temperature regime of the synthesis of the chromite – manganite. The type of crystal system and unit cell parameters were determined by the radiographic method. It is established that a complex mixed manganite is crystallized in the orthorhombic crystal system, the correctness of the results of X-ray studies of the manganite is confirmed by the good concordance between the experimental and calculated values ($10^4/d^2$), concordance between the values of X-ray and picnometer densities [15, 16].

Conclusions. Radiographic method determined the type of symmetry and the parameters of the elementary cells. It is revealed that chromite-manganites obtained by sol-gel method crystallize in the orthorhombic structure and correspond to the formulas $Y_{(1-X)}MeCr_{0,5}Mn_{0,5}O_3$(Me = Mg, Ba, Sr, x≈0,7).

Acknowledgement. *This article was prepared with the financial support of the grant of the Ministry of Education and Science of the Republic of Kazakhstan №AP05130165 "Development and physical basis of new crystal systems in the class of multiferroics".*

REFERENCES

[1] Lewis N.S., Nocera D.G. Electromicrobiology: An Emerging Reality – A Review // Proc. Natl. Acad. Sci. USA. 2006. N 103. P. 15729.

[2] Turner J.A. A Realizable Renewable Energy Future // Science. 1999. N 285. P. 687-689.

[3] Kreuter W., Hofmann H. Electrolysis: the important energy transformer in a world of sustainable energy // Int. J. Hydrogen Energy. 1998. N 23. P. 661-666.

[4] Singhal S.C., Kendall K. High-temperature Solid Oxide Fuel Cells: Fundamentals, Design and Applications // High-Temperature Solid Oxide Fuel Cells: Fundamentals, Design and Applications. Elsevier Science, Oxford, UK, 2003.

[5] Chroneos A., Yildiz B., Tarancon A., Parfitt D., Kilner J.A. Prediction of solid oxide fuel cell cathode activity with first-principles descriptors // Energy Environ. Sci. 2011. N 4. P. 3966-3970.

[6] Bockris J.O'M., Otagawa T. The Electrocatalysis of Oxygen Evolution on Perovskites // Elecrochem. Soc. 1984. N 131. P. 290-302.

[7] Man I.C., Su H.-Y., Calle-Vallejo F., Hansen H.A., Martнnez J.I., Inoglu N.G., Kitchin J., Jaramillo T.F., Nшrskov J.K., Rossmeisl J. Universality in Oxygen Evolution Electrocatalysis on Oxide Surfaces // ChemCatChem. 2011. N 3. P. 1159-1165.

[8] Skinner S.J. Recent advances in Perovskite-type materials for solid oxide fuel cell cathodes // Int. J. Inorg. Mater. 2001. N 3. P. 113-121.

[9] Haile S.M. Fuel cell materials and components // Acta Mater. 2003. N 51. P. 5981-6000.

[10] Jacobson A.J. Materials for Solid Oxide Fuel Cells // Chem. Mater. 2010. N 22. P. 660-674.

[11] Suntivich J., Gasteiger H.A., Yabuuchi N., Nakanishi H., Goodenough J.B., Shao-Horn Y. Design principles for oxygen-reduction activity on perovskite oxide catalysts for fuel cells and metal-air batteries // Nat. Chem. 2011. N 3. P. 546-550.

[12] Hong W.T., Risch M., Stoerzinger K.A., Grimaud A., Suntivich J., Shao-Horn Y. Toward the rational design of non-precious transition metal oxides for oxygen electrocatalysis // Energy Environ. Sci. 2015. N 8. P. 1404-1427.

[13] Shabanova N.A., Sarkisov P.D. Osnovy zol-gel tehnologıı nanodispersnogo kremnezema. M.: IKTs «Akademknıga», 2004. 208 p.

[14] Kasenov B.K., Kasenova Sh.B., Sagıntaeva J.I. Dvoinye i troinye manganity, ferrity i khromity elochnyh, elochnozemelnyh ı redkozemelnyh metallov // M., 2017.

[15] Mataev M.M., Saxena S.M., Patrin G.S., Tursinova Zh.Y., Kezdikbayeva A.T., Nurbekova M.A., Baitasheva G.U. Manganite synthesis by different methods // Oriental jornal of chemistry. 2018. N 34(3). P. 1312-1316.

[16] Mataev M.M., Patrin G.S., Tursinova Zh.Y., Abdraimova M.R.,Yurkin G.Yu. Synthesis and Magnetic Properties of crystals $Bi_2BaFe_4O_{10}$ // Journal of Siberian Federal University. Mathematics & Physics. 2018. N 11(4). P. 411-415.

Резюме

М. М. Матаев, Г. С. Патрин, К. Ж. Сейтбекова,
Ж. И. Турсинова, М. Р. Абдраймова

ХРОМИТТІ-МАНГАНИТТЕРДІ СИНТЕЗДЕУ
ЖӘНЕ РЕНТГЕНҚҰРЫЛЫМДЫ ЗЕРТТЕУ

Жұмыста $Y_{(1-X)}MeCr_{0,5}Mn_{0,5}O_3$(Me = Mg, Ba, Sr, x≈0,7) құрамды жаңа хромитті-манганиттер фазасы золь–гельәдісімен синтезделген, рентгендік зерттеу жұмысы жүргізілген. Бастапқы материалдар ретінде хром оксиді, марганец оксиді, иттрий оксиді, металл карбонаттары, лимон қышқылы және глицерин қолданылды. Лимон қышқылы мен глицеринді тұндырғыш ретінде пайдалану үлгілердің монофазалығына оң әсер етеді. Алынған тұнба 600–1100°С температура диапазонында гомоге-низациялық күйдіруге ұшырап, үлгілердің бірігу деңгейіне жетуі рентген дифроктаграммалары негізінде бақыланды. Рентген фазалық талдау нәтижесі бойыншахромитті-манганиттер Pbnm (62) кеңістіктік тобында орторомбтық перовскит құрылымы бойынша индицирленген және келесі ұяшық параметрлеріне ие: $Y_{(1-x)}MgCr_{0,5}Mn_{0,5}O_3$, (x≈0,7), –a=5.557, b=7.515, c=5.252 Å, Z = 4; $Y_{(1-x)}BaCr_{0,5}Mn_{0,5}O_3$, (x≈0,7), –a=9.102, b=5.533, c=7.330 Å, Z = 4; $Y_{(1-x)}SrCr_{0,5}Mn_{0,5}O_3$, (x≈0,7), –a=7.109, b=7.436, c=6.756 Å, Z = 4.

Түйін сөздер: хром кешені, золь-гельді процестер, кристалды құрылымдар, нанокұрылымдар, допирлеу, рентгендік дифракция.

Резюме

М. М. Матаев, Г. С. Патрин, К. Ж. Сейтбекова,
Ж. И. Турсинова, М. Р. Абдраймова

СИНТЕЗ И РЕНТГЕНОСТРУКТУРНОЕ ИССЛЕДОВАНИЕ ХРОМИТО-МАНГАНИТОВ

В работе представлено рентгенографическое исследование синтезированных золь-гель методом новых хромито-манганитовых фаз состава: $Y_{(1-X)}MeCr_{0,5}Mn_{0,5}O_3$ (Me = Mg, Ba, Sr, x ≈ 0,7).

В качестве исходных материалов использовались оксид хрома, оксид марганца, оксид иттрия, карбонаты металлов, лимонная кислота и глицерин. Показано, что использование лимонной кислоты и глицерина в качестве осадителя положительно влияет на монофазность образцов. Осадки подвергались гомогенизирующему обжигу в диапазоне температур 600– 1100 °С, достижения уровня спекания образцов контролировали на основании профилей рентгеновских дифроктаграмм. Все линии рентгеновского отражения успешно индексированы в искаженной перовскитоподобной орторомбической структуре с пространственной группой: Pbnm (62) и со следующими параметрами: $Y_{(1-x)}MgCr_{0,5}Mn_{0,5}O_3$, (x≈0,7), –a=5.557, b=7.515, c=5.252 Å, Z=4; $Y_{(1-x)}BaCr_{0,5}Mn_{0,5}O_3$, (x≈0,7), –a=9.102, b=5.533, c=7.330 Å, Z=4; $Y_{(1-x)}SrCr_{0,5}Mn_{0,5}O_3$, (x≈0,7), –a=7.109, b=7.436, c=6.756 Å, Z=4.

Ключевые слова: комплекс хрома, золь-гель процессы, кристаллические структуры, наноструктуры, легирование, дифракция рентгеновских лучей.